Eur. Phys. J. D **14**, 361–366 (2001)

THE EUROPEAN PHYSICAL JOURNAL D

EDP Sciences

Electron temperature measurement in a surface-wave-produced argon plasma at intermediate pressures

C. Lao[1], J. Cotrino[2,a], A. Palmero[2], A. Gamero[1], and A.R. González-Elipe[3]

[1] Departamento de Fisica Aplicada, Universidad de Córdoba, Córdoba, Spain
[2] Departamento de Fisica Atómica, Molecular y Nuclear, Universidad de Sevilla, 411080 Sevilla, Spain
[3] Instituto de Ciencias de Materiales, Isla de la Cartuja, 411080 Sevilla, Spain

Received 24 July 2000 and Received in final form 19 January 2001

Abstract. The main objective of this work is to obtain the electron temperature in an argon surface-wave-produced plasma column at intermediate gas pressures. After proving that argon upper excited states remain in Excitation Saturation Balance, the value of electron temperature along the plasma column has been obtained using a modified Saha equation and a corrected Boltzmann-plot. Moreover, the electron energy distribution function has been verified to be nearly Maxwellian in a 0.8–2.8 torr intermediate pressure range.

PACS. 52.70.-m Plasma diagnostic techniques and instrumentation – 52.70.Kz Optical (ultraviolet, visible, infrared) measurements – 52.80.Pi High-frequency and RF discharges

1 Introduction

In recent years, the interest in high-frequency (hf) discharges have been renewed. In particular hf discharges sustained by traveling electromagnetic waves are used in science and industry due to their stability and good reproducibility over wide-range gas-discharge conditions [1]. These nonequilibrium plasmas are very efficient sources of active species (radicals, excited neutrals, ions, etc.) and their applications increase every year [2]. In the last 25 years, this new branch in the field of hf discharges, notably those sustained by a surface-wave propagation, has been extensively developed [3]. Surface-wave (sw) discharges have also been extensively modeled, probably more than any other hf discharge, and this modeling has furthermore been developed in a context where its conclusions could be extended to hf discharges in general.

Several theoretical works on sw discharges at different operating conditions and configurations have been performed by different groups (see Ref. [4] and references therein). These models take into account the plasma kinetic and the surface wave propagation along the plasma column. Also, they included the Boltzmann's transport equation to calculate the electron energy distribution function (EEDF), and an energy balance equation between charged and neutral gas particles. The solutions of these models point out that the most important quantities used to describe the plasma (electron density, absorbed power per electron, electron temperature, etc.) show an axial dependence along the plasma column [5]. In this paper, an experimental method has been applied in order to determine the axial electron temperature dependence in sw discharges, in the 0.2−2.8 torr pressure range.

A classic method to determine the electron temperature in low-pressure glow discharges is the Langmuir probe method [6]. Langmuir probes have been also used in microwave discharges produced by surface-wave [7]. Besides, in the last years, a great number of spectroscopic methods to measure the electron temperature in cold plasmas have been developed. In general, the discharge can be characterized using a two temperature formulation, one for the heavy particles (T_g) and the other for the light ones (T_e). This description needs a deep study of the problem to know the influence of each temperature on the system properties. Indeed, the translational energy of excited atoms is related with temperature T_g, but the electron population distribution on the atomic energy levels may contain information about T_e. Based on this fact, all the spectroscopic methods try to obtain the electron temperature using some information about the excited states population. In an ionization-recombination equilibrium with no transport, the electron temperature is represented by the exponential factor of the Saha equation. In this way, van der Sijde and van der Mullen proposed a method to obtain the electron temperature using a Maxwellian model to characterize the plasma kinetic [8].

[a] e-mail: cotrino@cica.es

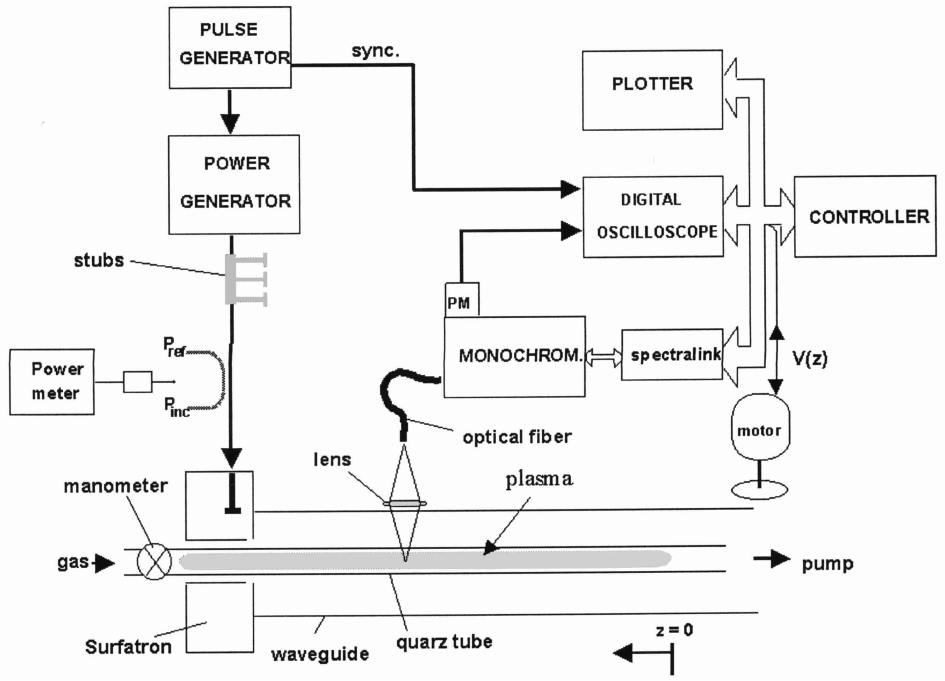

Fig. 1. Experimental setup.

In this paper, we make the distinction between Close-to-LTE plasmas (including P(artial) LTE plasmas) and Far-from-LTE plasmas. Close-to-LTE is defined

$$0.1 \leq b(1) = \frac{n(1)}{n^{\mathrm{s}}(1)} \leq 10,$$

here, $b(1)$ is the ratio of the ground state density, $n(1) = N$, to the density according to the Saha-equation, $n^{\mathrm{s}}(1)$. Values of $b(1) > 1$ refer generally to ionizing plasmas and $b(1) < 1$ to recombining ones. For a given excited level, described by an effective principal quantum number p, the condition $b(p) = n(p)/n^{\mathrm{s}}(p) = 1$ is an essential requirement to determine the electron temperature through a Boltzmann-plot. For plasmas with transport, the well known Griem criterion is not sufficient [9].

Far-from-LTE plasmas can be characterized through different kinetic balances that receive different names in the bibliography: Corona Balance, Excitation Saturation Balance (ESB) for ionizing plasmas, Capture Radiative Cascade Balance (CRC) for recombining plasmas, etc. In these cases, the excited levels are not in Saha-equilibrium and the use of Boltzmann-plots leads to erroneous temperature determination.

In this paper, we have used the method proposed by van der Sijde and van der Mullen to calculate the electron temperature along the plasma column for an argon surface-wave produced plasma at intermediate pressures [8]. So, the populations of the higher-lying levels in the excitation scheme have been measured. Moreover, through these values, we have deduced that the upper excited levels in the discharge can be described assuming an Excitation-Saturation-Balance regime. At last, as the spectroscopy method assumed a Maxwellian description for the electrons, we have discussed the shape of the EEDF in these conditions to assure the validity of the results.

This paper is organized as follows. In the next section, the experimental procedure is explained. Section 3 is devoted to show the theoretical background used to determine the electron temperature variation along the plasma column. Finally, in Section 4, we present a discussion of the results and the conclusions.

2 Experimental setup

2.1 Microwave plasma source

The argon plasma was generated by a microwave plasma source which has been described in detail elsewhere [10]. Essentially, the microwave power was coupled to the plasma by a device that produce a surface-wave plasma. Surface-wave plasma columns have been produced in a Pyrex cylindrical tube ($R_{\mathrm{inner}} = 0.45$ cm, $R_{\mathrm{ext}} = 0.6$ cm, $\varepsilon_{\mathrm{d}} = 4.8$) by coupling the 2.45 GHz hf energy *via* a surfatron-type launcher to produce the azimuthally symmetric ($m = 0$) mode. The tube was surrounded by a metal screen of radius $R_{\mathrm{m}} = 2.0$ cm. Argon gas was used in the discharge at five work pressures, 0.2, 0.8, 1.1, 1.8 and 2.8 torr (low and intermediate domain), being the incident power at the gap in the discharge fixed at 100 W. The length of the columns ranged from 40 to 58 cm, depending on the gas pressure.

Compared with their ends, columns produced by different powers are equivalent in such a way, that the total power dissipated producing the discharge is not a relevant parameter. Figure 1 shows a block diagram of the

discharge and the diagnostic setup which also includes optical elements for spectroscopic measurements (lens, optical fiber, AD converter, monochromator, etc.). A PC controlled the whole sequence of measurements.

2.2 Optical emission spectroscopy

For optical emission spectroscopy, we used a scanning 1 m monochromator (Jobin Yvon HR1000). It was equipped with a holographic grating with 1200 lines cm^{-1}, giving a wavelength resolution of 0.01 nm, and a photomultiplier (Hamamatsu R928). The light emission spectrum was measured as a function of gas pressure, at different microwave power levels, for different position along the column. In this way, after calibrating, we obtain the absolute value of the higher-lying excited level populations. The light was collected at different axial positions from the surfatron using a fiber optic (Fig. 1). It must be noted that the spectroscopic intensities were integrated over the line of sight, limiting the spatial resolution.

3 Temperature measurement in Far-from-LTE plasmas

3.1 Saha equation

In the last years, a theoretical background for two temperature plasmas has been developed, and different versions of the Saha equation has been deduced, taking into account the gas and electron temperature. In this way, if we consider the reaction $X^+ + e + e \leftrightarrow X_p + e$ (being p the effective principal quantum number), the chemical equilibrium condition, $\sum_i \nu_i \mu_i = 0$, must be used, where ν_i is the stoichiometric coefficient of the specie i and μ_i the chemical potential, which depends on both temperatures (gas and electron temperature). This method of calculating the Saha equation has some theoretical problems as we are implicitly negating the equilibrium condition when assuming a two temperature formulation. Richley and Tuma [11], from a kinetic point of view, pointed out that the concept of minimum free energy is not valid in multiple-temperature plasma. Some years later, van der Sanden *et al.* assumed a new definition through thermodynamic principles [12]. This formulation seems to be better for Tanaka *et al.* [13] and Han *et al.* [14]. Assuming such definition, a new condition, $\sum_i \nu_i \mu_i / T_i = 0$, was obtained [15]. With this result, the Saha equation

$$\frac{n_\mathrm{e} n_+}{n^\mathrm{s}(p)} = \frac{g_\mathrm{e} g_+}{g_p} \left[\frac{2\pi m_\mathrm{e} k_\mathrm{B} T_\mathrm{e}}{h^2}\right]^{3/2} \mathrm{e}^{-\frac{E_{p\lambda}}{k_\mathrm{B} T_\mathrm{e}}}, \qquad (1)$$

where g_e, g_+ and g_p are the statistical weight of each state, and $E_{p\lambda}$ the ionization energy from the excited level, remains independent on the gas temperature in the experimental conditions of this paper.

3.2 Electron temperature calculation

The Excitation Saturation Balance (ESB) in collisional-radiative models is characterized by excitation mechanism dominated by collisional processes with electrons, namely a ladder-like excitation mechanism from lower to higher levels in ionizing plasmas. Three-body recombination is not still important and the Saha-equation is not valid for levels in ESB. The Saha population density can be related to the nonequilibrium one in the form [16]

$$n(p) = b(p) n^\mathrm{s}(p).$$

Making a study of the cross-sections of the model and using a Maxwellian description for the electrons, $b(p)$ can be written as [17]

$$b(p) = b_0 p^{-m} + 1,$$

here, b_0 is a positive constant for ionizing plasmas (negative for recombining ones). As it has been probed, if $m > 5$ we can assure that the plasma can be described through an ESB balance. Using

$$\frac{n^\mathrm{s}(p)}{n_\mathrm{t}} = \frac{n(p)}{b(p) n_\mathrm{t}} = \frac{g_p \exp\left(-E_p / k_\mathrm{B} T_\mathrm{e}\right)}{Z(T_\mathrm{e})},$$

and

$$I_{pq} = \frac{n(p) A_{pq} hc}{\lambda_{pq} 4\pi},$$

where n_t is the total population density, $Z(T_\mathrm{e})$ the partition function, E_p the energy of the p-level, I_{pq} the line intensity per solid angle for the transition p–q, A_{pq} the Einstein coefficient for the transition and hc/λ_{pq} the energy, we can obtain

$$\ln\left(\frac{I_{pq}\lambda_{pq}}{A_{pq} g_p b(p)}\right) = \ln\left(\frac{n_\mathrm{t} hc}{4\pi Z(T_\mathrm{e})}\right) - \frac{E_p}{k_\mathrm{B} T_\mathrm{e}}, \qquad (2)$$

so that, a corrected Boltzmann-plot of $\ln(I_{pq}\lambda_{pq}/A_{pq} g_p b(p))$ against the excitation energy gives the desired temperatures value. For levels with $n(p) \gg n^\mathrm{s}(p)$ we can write $b(p) \simeq b_0 p^{-6}$, and the value of b_0 is not important. In Figure 2 we have represented $\ln(I_{pq}\lambda_{pq}/A_{pq} g_p)$ and $\ln(I_{pq}\lambda_{pq}/A_{pq} g_p b(p))$ against the excitation energy at a gas pressure of 0.2 torr. As we can note, the correction term changes drastically the results of the calculation.

On the other hand $m = 6$ is only an estimation and we do not know exactly its value. Using equation (2) we can write

$$\ln\left(\frac{I_{pq}\lambda_{pq}}{A_{pq} g_p}\right) = \ln\left(\frac{n_\mathrm{t} hc b_0}{4\pi Z(T_\mathrm{e})}\right) - m \ln p - \frac{E_p}{k_\mathrm{B} T_\mathrm{e}}, \qquad (3)$$

that allows us to perform a iterative method to calculate the best value of m. This method consists in

1. making a linear fit between $\ln\left(I_{pq}\lambda_{pq}/A_{pq} g_p\right)$ and $\ln p$ and obtaining an estimation of m;

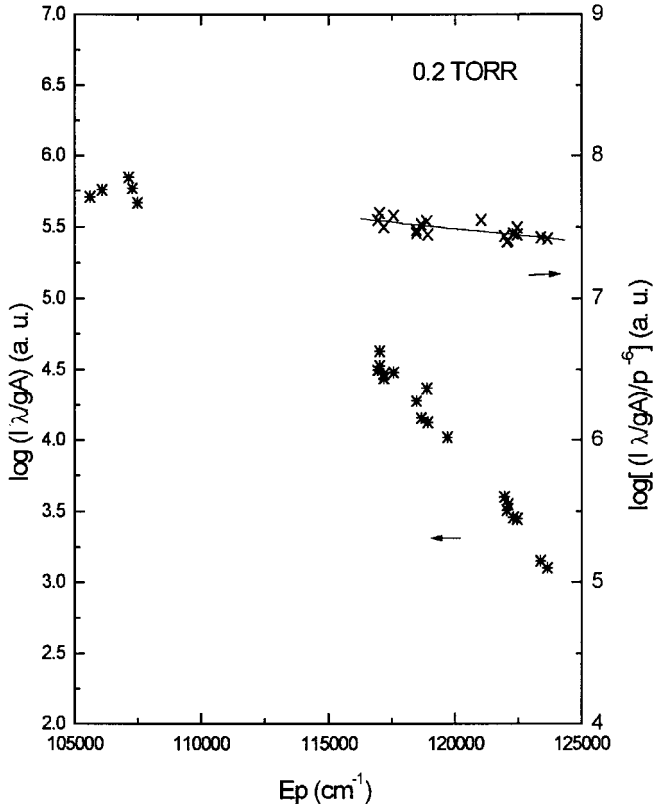

Fig. 2. Representation of $\ln \frac{I_{pq}\lambda_{pq}}{A_{pq}g_p}$ and $\ln \frac{I_{pq}\lambda_{pq}}{A_{pq}g_p b(p)}$ *versus* E_p.

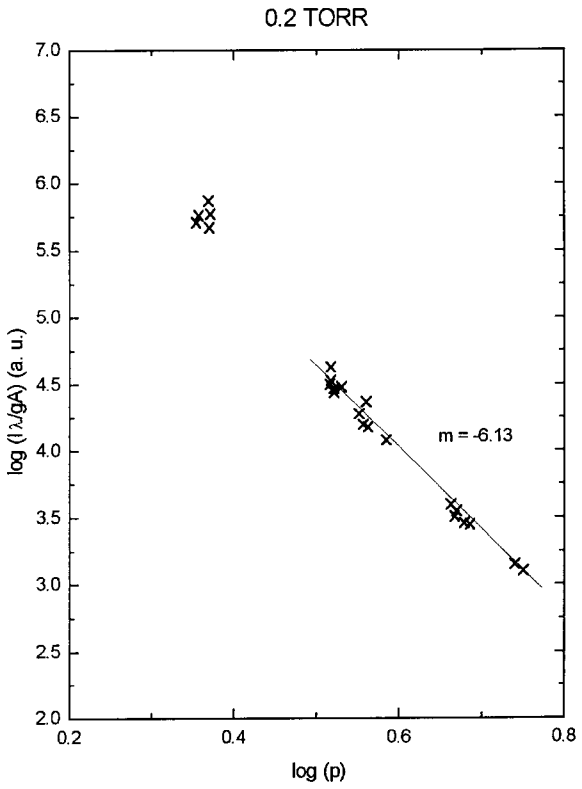

Fig. 3. Corrected population densities *versus* effective quantum number at a gas pressure of 0.2 torr.

2. obtaining the temperature T_e through a linear fit between $\ln(I_{pq}\lambda_{pq}/A_{pq}g_p) + m \ln p$ and E_p, taking into account the value of m;
3. obtaining a new value of m through a new linear fit between $\ln(I_{pq}\lambda_{pq}/A_{pq}g_p) + E_p/k_B T_e$ and $\ln p$. Using equation (3) and the value of T_e;
4. repeating the calculation from the second step until the temperature difference between two consecutive iterations becomes lower than 10%.

In Figures 3 and 4 we have represented these results at 0.2 and 2 torr, respectively. In both cases, we can check the good agreement between the corrected data and the linear fit.

We have represented the results in Figure 5, where the position z along the plasma refers to the end of the plasma column. In all the cases, the electron temperature seems to increase from the wave launcher gap to the column end, but the experimental uncertainty ($\sim 10\%$) does not allow to conclude such a dependency.

4 Discussion and conclusions

Although the T_e obtained values are, in general, in good agreement with other measures in the same experimental conditions [7], the method we have used makes some theoretical assumptions about the discharge kinetics. First of all, the order of magnitude of the electron density found

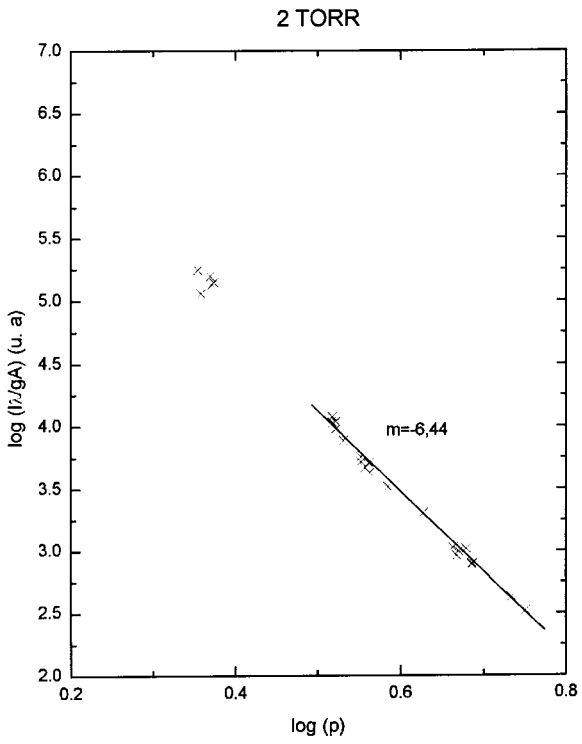

Fig. 4. Corrected population densities *versus* effective quantum number at a gas pressure of 2 torr.

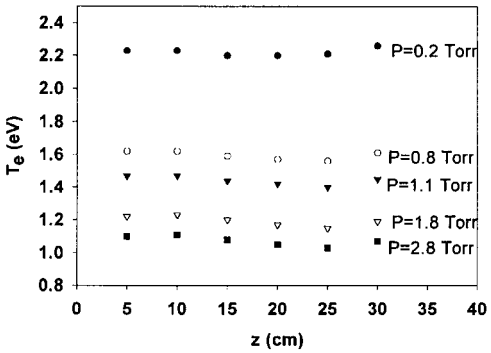

Fig. 5. Axial variation of the electron temperature at different gas pressures.

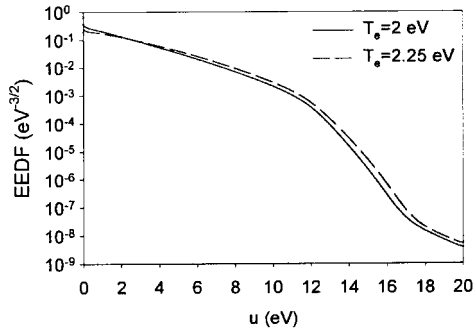

Fig. 6. Typical EEDFs calculated through the Boltzmann's Transport Equation at 2.8 torr.

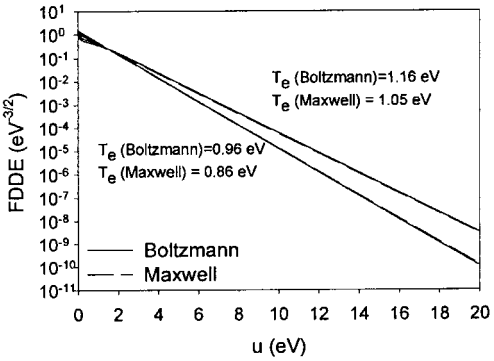

Fig. 7. Typical EEDFs calculated through the Boltzmann's Transport Equation at 0.2 torr.

in these discharges corroborates the results of this work [10]. Some years ago, Fujimoto [16] proved that the main mechanisms of populating and depopulating excited states would be the typical of a Corona Balance if the electron density values are lower than 10^{11} cm^{-3}. For electron densities between 10^{11} and 10^{15} cm^{-3} the system remains in a quasi-saturation balance as the excitation from the ground level might play an important role. At last, for electron densities higher than 10^{15} cm^{-3}, we find a complete saturation phase.

These limits are important since the external parameter, as the cylinder radius, gas pressure, incident wave power intensity at the gap, etc. determine the electron density value, and therefore, change the excitation mechanisms. In this work, we have found an ESB regime, coherent with the typical electron densities obtained in the experimental conditions (10^{11}–10^{13} cm^{-3}).

The main problem of accepting the proposed method to calculate the electron temperature is the assumption of Maxwellian EEDFs in the theoretical model. This function is very important to describe the electron properties and, in general, it has to be calculated solving the Boltzmann's transport equation. All the discharge populations and processes depend strongly on the EEDF shape. In this way, stepwise ionization is linked to the low energy part of the EEDF, as the excitation transition between two consecutive levels involves collisions with low energy electrons. On the other hand, the direct ionization from the ground level is linked to the high energy part of the EEDF since only high energy electrons are responsible of such process.

Solving the Boltzmann equation is difficult in general, but in the conditions of this work, it may be solved through the well-known two term approximation [18–21]. This approximation has been proved experimentally and has provided satisfactory results [7]. In general, it would be good to use Maxwellian EEDF but it has been proved that, strictly speaking, this situation is impossible in general [22]. Anyway, some situations have been found in which Maxwellian EEDF, can be appropriate to describe the electrons in an argon plasma, especially at high ionization degrees due to electron-electron interactions [19].

We have solved the Boltzmann's transport equation for some typical cases of electric field intensity, electron density and temperature at several pressures by using the ELENDIF code [24]. This code can treat inelastic and superelastic processes, electron-electron and electron-ion collisions, photon-electron (free-free) processes, attachment and recombination, ionization, and an external source of electrons. The code also computes the mean electron energy, drift velocity, diffusion coefficient, rate coefficients and energy flow rates for the processes included in the calculation.

In Figure 6 we have represented some EEDFs at 2.8 torr as a function of the electron kinetic energy $u = mv^2/2$ in typical experimental conditions [25]. The input values at this pressure were $T_g = 300$ K, $n_e = 5 \times 10^{12}$ cm^{-3} and fractional population of metastable states $n_m/n_1 = 10^{-5}$ [26]. The values of E_{eff}/N (where E_{eff} is the effective field intensity [27]) were chosen to obtain an electron temperature value close to the measured value: $E_{eff}/N(T_e = 1.16$ eV$) = 0.3$ Td and $E_{eff}/N(T_e = 0.96$ eV$) = 0.2$ Td. In these cases we have also represented the Maxwellian best fit for the tail, being the Maxwellian temperature very close to the Boltzmann (below 10%). As a conclusion it seems that the Maxwellian approximation can be appropriate to describe most of the electron properties and to evaluate the electron temperature. This approximation has been performed for several pressures, and holds for values above 0.8 torr. In Figure 7 we have represented the EEDF at a gas pressure of 0.2 torr. The input parameter values at this pressure were $T_g = 300$ K, $n_e = 10^{11}$ cm^{-3} and fractional population of metastable states $n_m/N = 10^{-5}$. The

values of $E_{\rm eff}/N$ were $E_{\rm eff}/N(T_{\rm e} = 2$ eV$) = 2.5$ Td and $E_{\rm eff}/N(T_{\rm e} = 2.25$ eV$) = 5$ Td. In these cases we can check that Maxwellian approximation is not valid, and so, we have to use the Boltzmann solution at this pressure.

Thus, we can assure that the temperature values obtained in this work are a good estimation of the electron temperature for gas pressures ranging from 0.8 to 2.8 torr, whereas, for lower pressures, they are only parameters used to describe the plasma kinetic through a Maxwellian model. In all the cases, the experimental uncertainty does not allow to determine the electron temperature axial behavior accurately, but it seems that there is a slightly axial dependence along the plasma column. This result has been also obtained in reference [23] through Langmuir probe techniques in similar experimental conditions. In that paper, the EEDFs were measured along the plasma column, and near-Maxwellian shapes were obtained. As a result, an axial variation of the electron temperature was pointed out, being more important at the end of the plasma column. On the other hand, there have been also theoretical investigations about the electron temperature axial dependence on electron density, and it seems that the stepwise ionization is the main mechanism that produces such behavior [28,29].

The advantage of using the presented method to measure the electron temperature is the non dependence on the gas temperature, whose value can also change along the plasma column length [30]. Anyway, the assumption for a constant electron temperature [31,32] is a valid approximation in this pressure range.

This work has been supported by the Dirección General de Investigación Cientifica y Técnica of Spain under Project No. MAT97-689.

References

1. M. Moisan, J. Hubert, J. Margot, G. Sauvé, Z. Zakrzewski, *Microwave Discharges: Fundamentals, Applications*, edited by C.M. Ferreira, M. Moisan (Plenum, New York, 1993), p. 1.
2. J. Paraszczak, J. Heidenreich, *Microwave Excited Plasmas*, edited by M. Moisan, J. Pellitier (Elsevier, Amsterdam, 1992), Chap. 15.
3. M. Moisan, J. Hubert, J. Margot, Z. Zakrzewski, *Advanced Technologies Based on Wave, Beam Generated Plasmas*, edited by H. Schlüter, A. Shivarova (Kluwer, Dordrecht, 1999), p. 23.
4. E. Benova, Ts. Petrova, A. Blagoev, I. Zhelyazkov, J. Appl. Phys. **84**, 147 (1998).
5. E. Tatarova, F.M. Dias, C.M. Ferreira, A. Ricard, J. Appl. Phys. **85**, 49 (1999).
6. I. Langmuir, H. Mott-Smith, Phys. Rev **28**, 727 (1926).
7. U. Kortshagen, A. Shivarova, E. Tatarova, D. Zamfirov, J. Phys. D: Appl. Phys. **27**, 301 (1994).
8. B. van der Sijde, J.A.M. van der Mullen, J. Quant. Radiat. Transfer **44**, 39 (1990).
9. H.R. Griem, *Principles of Plasma Spectroscopy* (Cambridge University Press, 1997).
10. A. Gamero, J. Cotrino, A. Sola, V. Colomer, J. Phys. D: Appl. Phys. **21**, 1275 (1988).
11. E. Richley, D.T. Tuma, J. Appl. Phys. **53**, 8537 (1982).
12. M.C.M van der Sanden, P.P.J.M. Schram, A.G. Peeters, J.A.M. van der Mullen, G.M.W. Kroesen, Phys. Rev. A **40**, 5273 (1989).
13. Y. Tanaka, Y. Yokomizu, M. Ishikawa, T. Matsumura, IEEE Trans. Plasma Sci. **25**, 991 (1997).
14. P. Han, X. Chen, H.P. Li, Chinese Phys. Lett. **16**, 193 (1999).
15. A. Gleizes, B. Chervy, J.J. González, J. Phys. D: Appl. Phys. **32**, 2060 (1999).
16. T. Fujimoto, J. Phys. Soc. Jap. **47**, 273 (1979).
17. J.A.M. van der Mullen, Phys. Rep. **191**, 109 (1990).
18. U. Kortshagen, H. Schlüter, A. Shivarova, J. Phys. D: Appl. Phys. **24**, 1571 (1991).
19. C.M. Ferreira, J. Loureiro, J. Phys. D: Appl. Phys. **17**, 1175 (1984).
20. U. Kortshagen, H. Schlüter, J. Phys. D: Appl. Phys. **25**, 644 (1992).
21. P.A. Sá, J. Loureiro, C.M. Ferreira, J. Phys. D: Appl. Phys. **25**, 960 (1992).
22. U. Kortshagen, J. Phys. D: Appl. Phys. **26**, 1230 (1993).
23. S. Grosse, H. Schlüter, E. Tatarova, Phys. Scripta **50** (1994).
24. ELENDIF77, CPC Program Library, `http://www.cpc.cs.qmb.ac.uk`.
25. A. Sola, A. Gamero, J. Cotrino, V. Colomer, J. Phys. D: Appl. Phys. **21**, 1112 (1988).
26. C. Lao, A. Gamero, A. Sola, T. Petrova, E. Benova, G.M. Petrov, I. Zhelyazkov, J. Appl. Phys. **87**, 7652 (2000).
27. C.M. Ferreira, J. Loureiro, J. Phys. D: Appl. Phys. **16**, 1611 (1983).
28. J. Cotrino, F.J. Gordillo-Vázquez, J. Phys. D: Appl. Phys. **28**, 1888 (1995).
29. E. Benova, Ts. Petrova, A. Blagoev, I. Zhelyazkov, J. Phys. D: Appl. Phys. **84**, 147 (1998).
30. J. Cotrino, A. Palmero, A. Barranco, A.G. Rodriguez-Elipe, submitted for publication.
31. V.M.M. Glaude, M. Moisan, R. Pantel, P. Leprince, J. Marec, J. Appl. Phys. **51**, 5693 (1980).
32. I. Zhelyazkov, V. Atanassov, Phys. Rep. **25**, 79 (1995).